Supplemental Information: The imprint of climate, topography and geology on the residence times of groundwater

Reed M Maxwell[1*], Laura E Condon[1], Stefan J Kollet[2], Katherine Maher[3], Roy Haggerty[4] and Mary Michael Forrester[1]
[1] Hydrologic Science and Engineering Program, Integrated GroundWater Modeling Center, Department of Geology and Geological Engineering, Colorado School of Mines, Golden, Colorado, USA
[2] Centre for High-Performance Scientific Computing in Terrestrial Systems, Institute for Bio- and Geosciences, Agrosphere (IBG-3), Research Centre Jülich, Jülich, DE
[3] Department of Geological Sciences, Stanford University, Stanford, California, USA
[4] College of Earth, Ocean and Atmospheric Sciences, Oregon State University, Corvallis, OR, USA

*correspondence to: Reed M Maxwell, rmaxwell@mines.edu

1. Model parameters for the flow simulation.

The particle tracking simulation presented in this work is based upon a flow simulation detailed in [*Maxwell et al.* 2015]. While the complete details and analysis of that work appear there, we provide a summary of some of the parameters here. Table S1 lists the hydraulic conductivity values used in Maxwell et al. [2015]. The domain is constructed using a terrain-following grid [*Maxwell* 2013] that extends to a total depth of 102 m below the ground surface across five vertical layers of 0.1, 0.3, 0.6, 1.0, and 100 m. Properties obtained from a national soil survey geographic database (SSURGO) were applied to the top two meters of the model domain. SSURGO has two sets of soil categories, the upper and lower soil horizons, which were applied to the top meter (the first three soil layers) and the meter below it (the fourth soil layer), respectively. Other soil properties such as van Genuchten parameters and porosity were obtained from Schaap and Leij [1998]. They applied pedotransfer functions to predict soil hydraulic properties from soil texture information and estimated the uncertainty in these predictions.

Hydraulic parameter distribution and values for the bottom 100 m of the model were derived from [*Gleeson et al.* 2011]. These values were adjusted using the empirically-derived relationships described in [*Fan et al.* 2007]. In this adjustment we assumed that the single 100m thick layer was comprised of the higher permeability material and lower permeability bedrock, with a bedrock thickness related to the local slope. For this analysis, we use the factor $\alpha = e^{-\frac{50}{f}}$, where $f = \frac{a}{1+b\sqrt{S_x^2+S_y^2}}$, to adjust hydraulic conductivity values. We chose $a = 20, b = 125,$ and a depth of 50 m to best represent the midpoint of the model's deepest geologic layer. We used discrete geometries in ParFlow (shown in Table 1) and facies in the subsurface indicator file were categorically reassigned based on α, with larger values of α corresponding to lower hydraulic conductivity. Thus, steeper slopes, which are assumed to demonstrate thinner regolith, will have comparatively lower conductivity than subdued terrain of the same lithology. Note that the variance and mean of the [*Gleeson et al.* 2011] values were shifted based upon a regional analysis [*Condon and Maxwell* 2014], in order to reflect a bulk conductivity value representative of coarse columnar discretization of the deeper subsurface. This process assumed that as hydraulic conductivity values were upscaled from point observations to the 1x1x0.1 km^3 volumes, small-scale, conductive flowpaths would dominate flow, pushing the effective values upward. In their regional analysis [*Condon and Maxwell* 2014] found that simulations conducted using the unaltered permeability values generated unrealistic surface flow. The resulting adjusted hydraulic conductivity values are shown in Table S1.

We recognize that our dataset for subsurface properties is not perfect. While many robust regional studies may provide excellent subsurface properties locally, as of yet no comprehensive large-scale parameter inputs exist. The current understanding of the full impact of weathered and fractured bedrock on hydraulic conductivity is limited at continental scales, and certainly our 102-m model thickness lacks the ability to represent confined aquifer systems and flow paths deeper than the extent of our model domain. These shortcomings in hydrogeological information will likely influence computation of travel times, and thus the datasets should be continuously improved as new information becomes available.

2. Comparison of ages for two steady-state models at varying resolution over a small, headwaters basin.

Computation of early travel times is dependent upon spatial discretization fine enough to describe local hydrogeologic properties. Because our model does not capture topography, hydraulic parameters and river channel geometry below the 1-km grid spacing, we have conducted a focused comparison of our results with those of a high-resolution simulation of a small, (25 km^2) headwaters basin that uses same flow and particle tracking framework. This comparison should serve as a grid convergence test to understand how travel-time distributions are altered with a coarser resolution model. The residence time distribution of the East Inlet watershed, in Colorado, USA, simulated by the current study (subsampled directly from the results shown in Figure 1) and a higher-resolution (20m laterally) integrated hydrologic model with a much more detailed geological model [*Engdahl and Maxwell* 2015] were compared. Note that both models are steady-state flow simulations with transient particle tracking. Figure S1 plots the results of this comparison. In this figure, we see that the capture of early residence times is likely associated with shorter flow paths not resolved by a 1-km spatial resolution. However, transit times less than one year comprise less than 4% of all ages in the 20m-resolution simulation, suggesting that these early times do not significantly contribute to the residence time distributions of major river basins. This figure also shows broad agreement between the two models, something that is somewhat surprising given that East Inlet only comprises 25 cells of the coarse resolution of CONUS simulation. Nevertheless, given the conclusions drawn from the CONUS simulation at very large spatial scales, comprising hundreds of thousands to millions of square kilometers, we feel this comparison serves to provide additional confidence in our large-scale residence time simulations.

Table S1. Indicators and hydraulic conductivity values used for the flow simulation, used as the basis for the particle tracking simulation.

Unit Indicator	Classification	Ks
		m/h
SURGO Classifications		
1	SAND	2.69E-01
2	LOAMY SAND	4.36E-02
3	SANDY LOAM	1.58E-02
4	SILT LOAM	7.58E-03
5	SILT	1.82E-02
6	LOAM	5.01E-03
7	SANDY CLAY LOAM	5.49E-03
8	SILTY CLAY LOAM	4.68E-03
9	CLAY LOAM	3.39E-03
10	SANDY CLAY	4.78E-03
11	SILTY CLAY	3.98E-03
12	CLAY	6.16E-03
13	ORGANIC MATERIAL	5.01E-03
Gleeson et al.		
21	f.g. sil. Sedimentary	2.00E-02
22	sil. Sedementary	3.00E-02
23	crystalline	4.00E-02
24	f.g. unconsolidated	5.00E-02
25	unconsolidated	6.00E-02
26	c.g. sil sedimentary	8.00E-02
26	volcanic	8.00E-02
27	carbonate	1.00E-01
28	c.g. unconsolidated	2.00E-01
Bedrock		
19	Bedrock 1	5.00E-03
20	Bedrock 2	1.00E-02

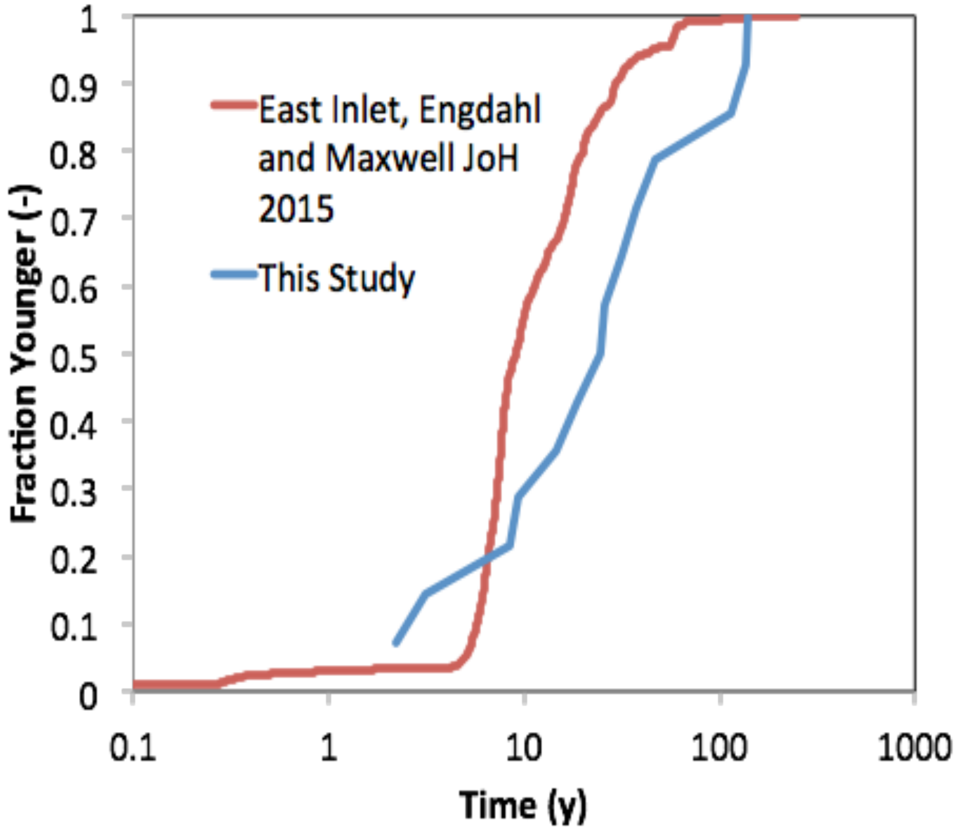

Figure S1. Comparison of *Engdahl and Maxwell 2015* with the results of the current study over the East Inlet Watershed in Colorado, USA.

References:

Condon, L. E. and R. M. Maxwell (2014). "Feedbacks between managed irrigation and water availability: Diagnosing temporal and spatial patterns using an integrated hydrologic model." Water Resources Research **50**(3): 2600-2616.

Engdahl, N. B. and R. M. Maxwell (2015). "Quantifying changes in age distributions and the hydrologic balance of a high-mountain watershed from climate induced variations in recharge." Journal of Hydrology **522**: 152-162.

Fan, Y., G. Miguez-Macho, C. P. Weaver, R. Walko and A. Robock (2007). "Incorporating water table dynamics in climate modeling: 1. Water table observations and equilibrium water table simulations." Journal of Geophysical Research-Atmospheres **112**(D10): -.

Gleeson, T., L. Smith, N. Moosdorf, J. Hartmann, H. H. Dürr, A. H. Manning, L. P. H. van Beek and A. M. Jellinek (2011). "Mapping permeability over the surface of the Earth." Geophysical Research Letters **38**(2): L02401.

Maxwell, R. M. (2013). "A terrain-following grid transform and preconditioner for parallel, large-scale, integrated hydrologic modeling." Advances in Water Resources **53**: 109-117.

Maxwell, R. M., L. E. Condon and S. J. Kollet (2015). "A high-resolution simulation of groundwater and surface water over most of the continental US with the integrated hydrologic model ParFlow v3." Geoscientific Model Development **8**: 1-15.

Schaap, M. G. and F. J. Leij (1998). "Database-related accuracy and uncertainty of pedotransfer functions." Soil Science **163**(10): 765-779.